RNA Biology 9:10, 1288–1301; October 2012; © 2012 Landes Bioscience

The 70S ribosome modulates the ATPase activity of *Escherichia coli* YchF

Marion Becker,[1,†] Katherine E. Gzyl,[1] Alvin M. Altamirano,[1] Anthony Vuong,[1] Kirstin Urbahn[1] and Hans-Joachim Wieden[1,2,*]

[1]Department of Chemistry and Biochemistry; University of Lethbridge; Lethbridge, AB Canada; [2]Alberta RNA Research and Training Institute; University of Lethbridge; Lethbridge, AB Canada

[†]Current affiliation: Department of Physics; University of Alberta; Edmonton, AB Canada

Keywords: YchF, universally conserved P-loop ATPase, HAS-ATPase, molecular switch, ribosome, ATPase activity, ATPase activating factor, Michaelis-Menten kinetics, *Escherichia coli*, RNA-binding protein

Abbreviations: NTPase, nucleoside triphosphatase; K_D, equilibrium dissociation constant; ATP/ADP, adenosine triphosphate/adenosine diphosphate; GTP/GDP, guanosine triphosphate/guanosine diphosphate; His-tag, hexahistidine-tag; k_{cat}, rate of catalysis or turnover number; K_M, Michaelis-Menten constant; RNA, ribonucleic acid; AAF/GAF, ATPase/GTPase activating factor; RGS, regulators of G protein signaling; P-loop, phosphate binding loop; wt, wild type; TGS domain, (ThrRS, GTPase, SpoT domain); G domain, GTP binding domain; A domain, α-helical domain; HAS-GTPase, hydrophobic amino acid substituted for catalytic glutamine; ADPNP, adenylyl-β-imidodiphosphate; FRET, fluorescence resonance energy transfer; mant, 2'(3')-O-(N-methylanthraniloyl); ITC, isothermal titration calorimetry; kDa, kilodalton; MDa, megadalton; SDS, sodium dodecyl sulfate; PAGE, polyacrylamide gel electrophoresis; RNase A, ribonuclease A; DNase 1, desoxyribonuclease 1; GFP, green fluorescent protein; B_{max}, maximal binding; v_{max}, maximal rate; k_1, on-rate; k_{-1}, off-rate; RA-GTPase, ribosome assembly GTPase; NEF, nucleotide exchange factor; ds, double-stranded; NAD/NADH, Nicotinamide adenine dinucleotide; P_i, inorganic phosphate; CoA, Coenzyme A; ROS, reactive oxygen species; LB medium, Luria Bertani medium; OD_{600}, optical density at 600 nm; IPTG, Isopropyl β-D-1-thiogalactopyranoside; bp, base pairs; MW, molecular weight; Tris, Tris(hydroxymethyl)-aminomethane; SD, standard deviation; PMSF, phenylmethylsulfonyl fluride; DTT, dithiothreitol; MWCO, molecular weight cut off; EDTA, Ethylenediaminetetraacetic acid; PDB, Protein data bank; V_o, void volume; SEC, size exclusion chromatography

YchF is one of two universally conserved GTPases with unknown cellular function. As a first step toward elucidating YchF's cellular role, we performed a detailed biochemical characterization of the protein from *Escherichia coli*. Our data from fluorescence titrations not only confirmed the surprising finding that $YchF_{E.coli}$ binds adenine nucleotides more efficiently than guanine nucleotides, but also provides the first evidence suggesting that YchF assumes two distinct conformational states (ATP- and ADP-bound) consistent with the functional cycle of a typical GTPase. Based on an in vivo pull-down experiment using a His-tagged variant of YchF from *E. coli* ($YchF_{E.coli}$), we were able to isolate a megadalton complex containing the 70S ribosome. Based on this finding, we report the successful reconstitution of a YchF•70S complex in vitro, revealing an affinity (K_D) of the $YchF_{E.coli}$•ADPNP complex for 70S ribosomes of 3 μM. The in vitro reconstitution data also suggests that the identity of the nucleotide-bound state of YchF (ADP or ATP) modulates its affinity for 70S ribosomes. A detailed Michaelis-Menten analysis of YchF's catalytic activity in the presence and the absence of the 70S ribosome and its subunits revealed for the first time that the 70S ribosome is able to stimulate YchF's ATPase activity (~10-fold), confirming the ribosome as part of the functional cycle of YchF. Our findings taken together with previously reported data for the human homolog of YchF (hOLA1) indicate a high level of evolutionary conservation in the enzymatic properties of YchF and suggest that the ribosome is the main functional partner of YchF not only in bacteria.

Introduction

Protein expression is a central process in all cellular life, and the majority of ubiquitous genes code for components of the translation system like ribosomal proteins, aa-tRNA synthetases, translation factors, proteins involved in polypeptide secretion and RNA and protein modification enzymes.[1] Several of these proteins are GTP-binding proteins (G proteins) that cycle between a GTP-bound "on" and a GDP-bound "off" state. In general, G proteins regulate a variety of cellular processes by coupling GTP hydrolysis to a universal conformational change which controls interaction with target molecules.[2] Comparative genomic studies have identified eight conserved GTPases present throughout all domains of life: EF-Tu, EF-G, IF-2, Ffh, FtsY, YihA, HflX

*Correspondence to: Hans-Joachim Wieden; Email: hj.wieden@uleth.ca
Submitted: 07/27/12; Revised: 09/05/12; Accepted: 09/08/12
http://dx.doi.org/10.4161/rna.22131

and YchF (*E. coli* naming).[3] The eight proteins phylogenetically cluster into four main GTPase families, namely the translation factor group (EF-Tu, EF-G and IF-2), the FtsY/Ffh group (FtsY, Ffh), the Era group (YihA) and the Obg group (HflX, YchF).[3] Increasing evidence indicates that, in addition to EF-Tu, EF-G, IF-2, FtsY and Ffh whose ribosome-associated functions have been extensively studied, the cellular roles of YchF, HflX (and YihA) are also related to the ribosome.[4-11] The GTP/GDP cycle of the three translation factors (EF-Tu, EF-G and IF2) is tightly regulated by the ribosome which acts as a GTPase activating factor (GAF) that highly stimulates their GTPase activity (**Table S1**).[12] Ffh and FtsY are involved in co-translational membrane targeting of proteins.

Comparatively few studies have addressed the cellular roles and biochemical properties of YihA, HflX and YchF. YihA has been shown to be essential for cell viability in *E. coli* and *B. subtilis*.[13,14] The protein binds GDP and GTP with low micromolar affinities and has been reported to have an extremely low intrinsic GTPase activity.[15] Similar to EF-Tu, EF-G, IF-2, Ffh and FtsY the cellular function of HflX seems to be ribosome-related. HflX proteins from different organisms bind to 50S and 70S ribosomes in vivo and in vitro and both the 50S and 70S ribosomes highly stimulate the GTPase activity of HflX.[16,17]

On the other hand, our understanding of the function, the molecular interaction partners, and properties of YchF is surprisingly poor. The fact that members of the YchF gene family have been found in every genome sequenced so far suggests its early emergence in evolution and a crucial function within the cell.[4,18] Furthermore, YchF exhibits a very high sequence conservation between kingdoms (*Escherichia coli* to *Homo sapiens* 45% identity and 62% similarity), which is typical for proteins of high functional conservation such as ribosomal proteins.[18] YchF has been reported to be essential in *Staphylococcus aureus*[5] and disruption of the *ychF* gene in *E. coli* results in growth retardation and filamentation at elevated temperatures.[13] Several studies have suggested that the protein participates in different processes such as protein translation,[5-7,19] ribosome biogenesis,[8] regulation of iron utilization in *Brucella melitensis* and *Vibrio vulnificus*,[20,21] protein degradation in yeast and *Trypanosoma cruzi*,[6,22] infection defense response in rice,[23] and stress response.[24-27] In addition, the human homolog of YchF, hOLA1 (human Obg-like ATPase 1), is overexpressed in different cancers like colon, rectum, ovary, lung, stomach and uterus indicating that the protein may have an important regulatory role.[27]

Crystal structures of YchF proteins from *Hemophilus influenza*, *Thermus thermophilus*, *Schizosaccharomyces pombe* and *Homo sapiens* have been solved.[19,28-30] YchF is composed of three domains, an N-terminal P-loop GTPase-domain, an α-helical coiled-coil insertion (A-domain) and a C-terminal TGS (ThrRS, GTPase, SpoT) domain, often found in RNA-binding proteins (**Fig. 1**). Overall, the protein assumes a crab-like structure in which the A-domain and the TGS-domain are separated by a 20 Å wide cleft. Positively charged residues cluster at the inner surface of the central cleft and were suggested to be a binding site for double-stranded nucleic acids.[19]

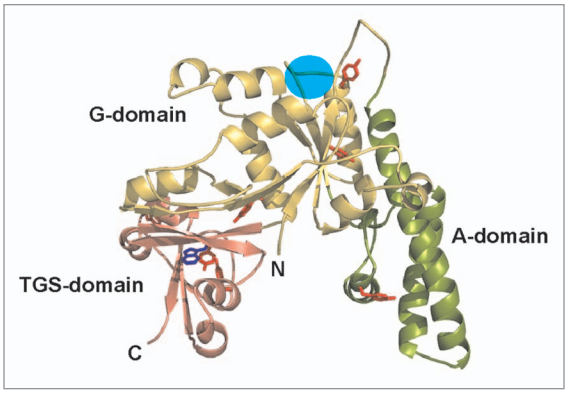

Figure 1. Homology model of *E. coli* YchF generated with SWISS-MODEL[58,59] using the structure of YchF from *Hemophilus influenzae* (PDP accession code: 1JAL)[19] as template and the amino acid sequence of *E. coli* YchF (Uniprot accession code: Q8F106). YchF proteins are composed of three domains, an N-terminal G-domain (residues 1 to 118 and 203 to 278; yellow), an α-helical coiled-coil insertion called the A-domain (residues 119 to 202; green) and a C-terminal TGS-domain (279 to 363, salmon). The nucleotide binding site as suggested by different crystal structures[28,29] is indicated by a blue sphere. Tyrosine (red) and tryptophan (blue) residues are depicted as sticks, and N- and C-terminal ends of the protein are indicated by an N and C, respectively.

Comparison of YchF crystal structures revealed a very high structural similarity among proteins from different organisms. The structural similarity is not only limited to the conserved G-domain, but strongest within the TGS domain. Based on the conserved G-motifs within YchF's G-domain, the protein was originally classified as a GTPase. Several studies have shown however, that YchF proteins can bind and hydrolyze both ATP and GTP, which was attributed to its unconventional G4 motif (NXXE instead of N/TKXD).[2] Another unusual feature of YchF is the lack of a highly conserved catalytic glutamine or histidine following the G3 motif ($D^{57}XXG^{60}$ Q^{61} in Ras) normally essential for GTPase activity. In YchF, the conserved glutamine is replaced by a leucine making it a member of the recently identified family of HAS-GTPase (hydrophobic amino acid substituted for catalytic glutamine).[31] The catalytic mechanism employed by these GTPases to hydrolyze GTP is not completely understood yet.[32,33]

In order to aid in the elucidation of YchF's cellular function, we performed a detailed biochemical characterization using *E. coli* YchF as a model system. We have characterized YchF's interaction with purine nucleotides and identified the 70S ribosome as a functional interaction partner of YchF in vivo and in vitro. For the first time, we demonstrate that the 70S ribosome stimulates YchF's ATPase activity, thereby acting as an ATPase activating factor (AAF). This makes YchF one of few ribosome-stimulated P-loop ATPases found in bacteria to date.

Results

***E. coli* YchF interaction properties with purine di- and triphosphates.** For many translational GTPases and ATPases the phosphorylation state (di-phosphate vs. tri-phosphate) of the

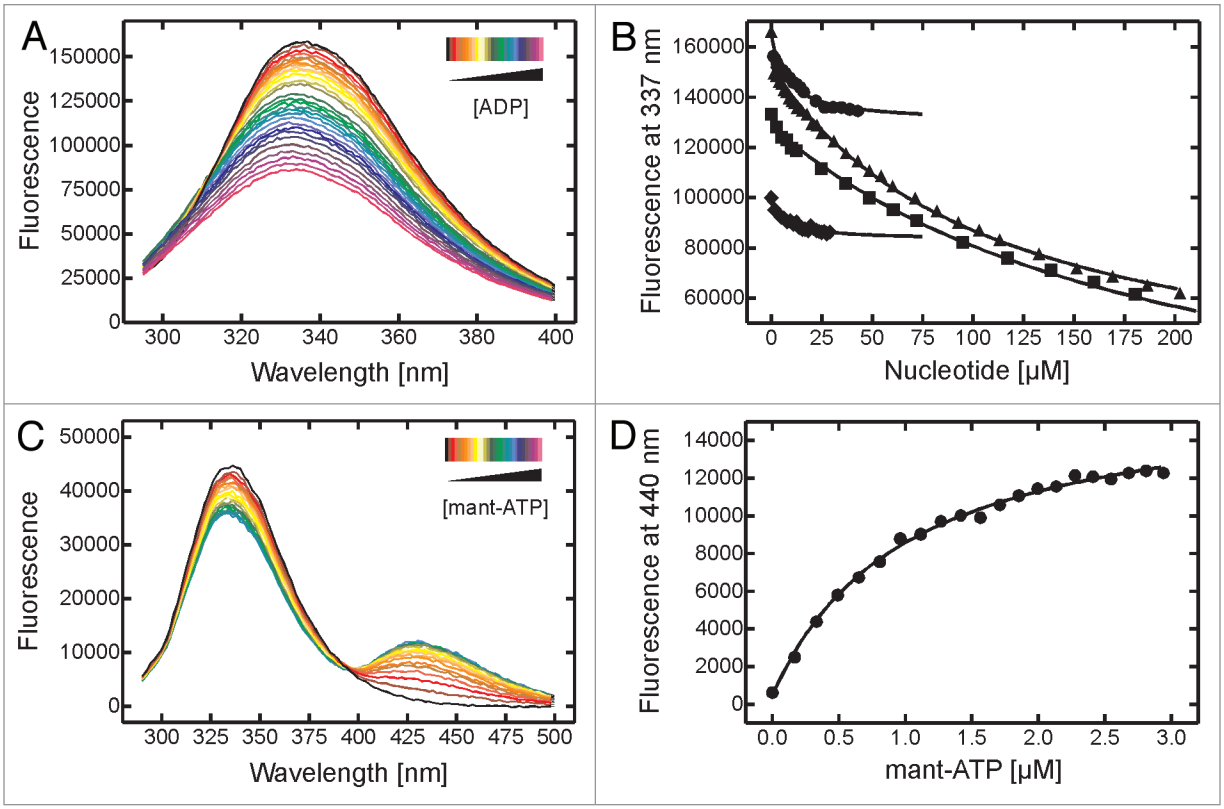

Figure 2. YchF binds adenine and guanine di- and triphosphates. Equilibrium fluorescence titrations of 1 μM YchF with increasing concentrations of ADP (**A**). Tyrosin and tryptophan fluorophors of YchF were excited at 280 nm and fluorescence emission spectra were detected from 295 to 400 nm. (**B**) Plot of the fluorescence signal at 337 nm against the concentrations of ADP(●), GDP (▲), GTP (■) and ADPNP (◆). (**C**) Titration of 1 uM YchF with increasing concentrations of mant-ATP. YchF was excited at 274 nm and emission spectra were recorded from 290 to 500 nm. (**D**) mant-ATP concentration dependence of the fluorescence resonance energy transfer (FRET) from YchF to the mant-group plotted at 440 nm. K_Ds were obtained by fitting the data with a hyperbolic function.

bound nucleotide determines their functional state on the ribosome. In order to characterize defined states of YchF, it is critical to have a detailed understanding of its nucleotide affinities, specificities and catalytic parameters. Several groups have shown that YchF binds both GTP and ATP, and that YchF from most organisms analyzed so far seems to utilize ATP more efficiently than GTP.[6,7,23,27,28,34] However, kinetic details for the interaction with GTP/GDP and ATP/ADP are only available for the human homolog hOLA1.[28] In order to provide a detailed description of these parameters also for a bacterial protein and to lay a foundation for functional work with *E. coli* YchF ($YchF_{E.coli}$), we have characterized its nucleotide specificity with respect to binding and hydrolysis (vide infra) of purine nucleotides.

First, we determined the affinities of $YchF_{E.coli}$ for ADP, ADPNP, ATP, GDP and GTP using equilibrium fluorescence titrations. $YchF_{E.coli}$ contains a single tryptophan residue (located in its TGS domain) and 7 tyrosine residues (3 in the TGS domain, 2 in the G-domain and 1 in the A-domain, **Fig. 1**), allowing us to monitor changes in YchF's intrinsic tryptophan fluorescence upon nucleotide addition (**Fig. 2A**, ADP titration). Upon excitation at 280 nm, YchF's fluorescence emission spectrum showed a maximal intensity at approximately 337 nm. As tryptophan fluorescence depends on the polarity of its environment (emission maximum of tryptophan in water is 353 nm), transferring the residue into a less polar environment leads to a blue shift of the emission maximum.[35] The observed 16 nm blue shift indicates that the tryptophan residue is at least partly shielded from the solvent, consistent with its position in the hydrophobic core of YchF's TGS domain. No shoulder was observed in the emission spectrum at 305 nm (emission maximum of tyrosine), suggesting that the fluorescence of the seven tyrosines is efficiently quenched, likely through fluorescence resonance energy transfer (FRET) from the tyrosine residues to the single tryptophan.[35]

Based on the performed titrations with the different nucleotides, the equilibrium dissociation constants (K_Ds) of $YchF_{E.coli}$ were determined for ADP, ADPNP, GDP and GTP by plotting fluorescence intensities at 337 nm against the nucleotide concentration. For all but one of the tested nucleotides (ATP, *vide infra*), the titrations resulted in fluorescence changes (decrease) that yielded affinities for the respective nucleotide in the micromolar range ($K_{D, ADP}$ = 14 ± 5 μM, $K_{D, ADPNP}$ = 9 ± 8 μM, $K_{D, GDP}$ = 151 ± 38 μM and $K_{D, GTP}$ = 206 ± 5 μM; summarized in **Table 1**). Interestingly, the amplitudes of the observed fluorescence changes differed significantly between adenine and guanine nucleotides, indicating binding of the nucleotides either to different sites on the protein or that they induce a different conformation of $YchF_{E.coli}$

Table 1. Equilibrium dissociation constants for *E. coli* YchF and purine nucleotides

Nucleotide	Signal	K_D [μM]	SD [μM]	rel. Amplitude (a.u.)	SD
ADP	YchF's intrinsic fluorophors	14	5	-34,960	6077
ADPNP	YchF's intrinsic fluorophors	9	8	-15,569	3960
ATP	YchF's intrinsic fluorophors	n.d.		no signal change	
GDP	YchF's intrinsic fluorophors	151	38	-107,074	32217
GTP	YchF's intrinsic fluorophors	206	5	-151,315	7390
mant-ADP	FRET to mant-group	4	2	10,565	5437
mant-ADPNP	FRET to mant-group	12	2	7,155	2367
mant-ATP	FRET to mant-group	0.9	0.4	14,987	7905

with different fluorescence properties (**Fig. 2B** and **Table 1**). Most strikingly, titration of $YchF_{E.coli}$ with ATP did not result in any detectable signal change, preventing us from determining the equilibrium binding constant for this nucleotide.

To further investigate ATP binding, we used the mant-labeled adenine nucleotide analogs to perform fluorescence resonance energy transfer (FRET) based equilibrium titrations with $YchF_{E.coli}$. In these experiments, $YchF_{E.coli}$'s intrinsic fluorophores (vide supra) were excited at 274 nm and emission spectra from 290 to 500 nm were recorded (**Fig. 2C**, mant-ATP). Addition of increasing concentrations of mant-nucleotides lead to a decrease of YchFs intrinsic tryptophan fluorescence at ~337 nm whereas a corresponding increase in mant-fluorescence with a maximum at about 440 nm was observed, consistent with the occurrence of FRET between tryptophan and the mant-group located on the nucleotide. To determine the K_D of YchF for the respective mant-nucleotides, we plotted the fluorescence at 440 nm against the nucleotide concentration and analyzed the data with a hyperbolic function (**Fig. 2D**). Equilibrium dissociation (K_D) constants derived from FRET titrations using mant-nucleotides were 4 ± 2 μM, 12 ± 2 μM and 0.9 ± 0.4 μM for mant-ADP, mant-ADPNP and mant-ATP, respectively (summarized in **Table 1**), similar to the affinities obtained using unlabeled nucleotides (**Table 1**) and demonstrate tight ATP binding. The determined affinities of $YchF_{E.coli}$ for ATP and GTP are in line with previously published values of hOLA binding to ATP (K_D ~8 μM) and GTP (K_D ~100 μM) obtained by isothermal titration calorimetry (ITC) and fluorescence polarization, suggesting conserved nucleotide binding properties between these evolutionarily distant protein homologs.[28]

YchF binds 70S ribosomes in vivo. Comparative genomic studies and experimental results suggest a ribosome related function for YchF.[4-11] Based on ribosome co-sedimentation experiments, these studies indicate that YchF from *E.coli* and *Trypanosoma cruzi* are able to interact with the ribosome as well as its two subunits. However, it is not clear if this interaction is functionally relevant. In order to identify potential interaction partners of YchF and to guide in the identification of the functionally relevant complex in vivo, we have performed pull-down experiments using a recombinant His-tagged variant of $YchF_{E.coli}$. We have overexpressed an N-terminally His-tagged $YchF_{E.coli}$ in *E. coli* and subsequently captured it from the cell lysate together with any bound cellular content using Ni^{2+}-Sepharose. After removing unspecifically bound proteins, any remaining Ni^{2+}-Sepharose-bound complexes were eluted and subsequently analyzed using size exclusion chromatography (Sephacryl S400, **Fig. 3A and B**). Two distinct peaks (A and B in **Figure 3A**) eluted from the initial size exclusion column. Interestingly, the higher molecular mass peak (A) eluting at approximately 60 mL, revealed a significantly higher absorbance ratio (A_{260}/A_{280}) when compared with the peak eluting around 95 ml, suggesting the presence of nucleic acids in peak A. To analyze the contents of peaks A and B, SDS-PAGE analysis and phenol:chloroform extractions with subsequent urea-PAGE analysis were performed. Phenol:chloroform extraction followed by urea-PAGE analysis revealed the presence of at least two distinct nucleic acids of roughly 200 and 2000 nucleotides in peak A, but none in peak B (**Fig. S1B**), consistent with the high A_{260}/A_{280} ratio. Treatment of the nucleic acids in Peak A with RNase A and DNase I, resulted in the degradation of the nucleic acid only upon RNase A treatment, suggesting that YchF is part of an RNA-containing complex in vivo (**Fig. S1C**). The SDS-PAGE analysis of peaks A and B revealed the presence of a protein with a molecular mass of ~40 kDa in both peaks, consistent with $YchF_{E.coli}$ eluting in each peak (**Fig. S1A**). In order to confirm the identity of this protein we performed a western blot analysis (slot-blot) with the content of peak A and B and probed for the presence of $YchF_{E.coli}$ using a $YchF_{E.coli}$-specific antibody (**Fig. 3C**, first SEC).

Calibration of the Sephacryl S400 column with purified $YchF_{E.coli}$, 70S, 50S and 30S ribosomes revealed that the complex in Peak A was of similar mass as the 70S ribosome (**Fig. 3B**). Subsequent SDS-PAGE analysis confirmed that in addition to $YchF_{E.coli}$ (and RNA) the complex (**Fig. 3D**, lane 3) also contained large and small ribosomal subunit proteins as well as two additional proteins with molecular masses of approximately 100 kDa and 50 kDa, respectively. To validate these observations, we utilized a $YchF_{E.coli}$-green fluorescent fusion protein (GFP)[36] as an independent method for the pull-down and subsequently purified the in vivo formed complex analog to the pull-down with $YchF_{E.coli}$ (*vide supra*). Similar to $YchF_{E.coli}$, $YchF_{E.coli}$-GFP contains a His-tag at its N-terminal end, whereas its C-terminal TGS-domain is fused to GFP (compare **Fig. 1**). Remarkably, also the 71 kDa $YchF_{E.coli}$-GFP fusion protein is capable of forming a stable high molecular weight complex containing 70S ribosomal

proteins and both the 50 kDa and 100 kDa proteins (**Fig. 3D**, lane 7).

In order to confirm the identities of the proteins found in the in vivo formed complex, protein bands were analyzed by mass spectrometry which verified the presence of 70S ribosomal proteins in complexes formed with both $YchF_{E.coli}$ and the $YchF_{E.coli}$-GFP fusion. Furthermore, the ~100 kDa protein was identified as 2-oxoglutarate dehydrogenase, the E1 component of the oxoglutarate dehydrogenase complex, involved in the citric acid cycle.[37] The ~50 kDa protein was identified as ATP-dependent RNA helicase RhlE which has previously been suggested to be involved in ribosome maturation.[38]

The intensity of the $YchF_{E.coli}$ and $YchF_{E.coli}$-GFP bands (**Fig. 3D**) varied between different pull-down experiments and suggests that more than one copy of the protein may be present. Interestingly, we repeatedly observed the band of the small ribosomal subunit protein S2 to be less intense than the other ribosomal protein bands suggesting a sub-stoichiometric representation in the complex. As ribosomal protein S2 is the last protein that associates during 30S assembly[39] this might indicate that $YchF_{E.coli}$ co-purified with not completely maturated ribosomes. However, removal of S2 during the pull-down canot be excluded.

Taken together, our results point at the 70S ribosome as the likely cellular interaction partner of $YchF_{E.coli}$. The small (approximately 20 pmol per gram of cells) yields of the YchF•70S complexes from different in vivo pull-downs, together with the underrepresentation of S2 in these ribosomes might indicate that tight binding of $YchF_{E.coli}$ only occurs to a specific subpopulation of ribosomes.

Reconstitution of the YchF•ribosome complex in vitro. In order to elucidate if a $YchF_{E.coli}$•70S complex can be reconstituted in vitro, we used purified $YchF_{E.coli}$, 70S ribosomes and ribosomal subunits (30S/50S) from *E. coli* in a ribosome sedimentation assay. To allow complex formation we first incubated recombinant $YchF_{E.coli}$ with purified 70S, 50S and 30S ribosomes in the presence and absence of various nucleotides at 37°C. To ensure that over 99% of $YchF_{E.coli}$ was in the nucleotide-bound state a concentration of 2 mM for the respective nucleotides was chosen, based on the dissociation constants determined above (**Table 1**). Furthermore, the use of 2 mM ATP also mimics the cellular ATP levels in *E. coli* during mid-log growth phase.[40] First, we examined the nucleotide-dependence of $YchF_{E.coli}$ binding by an incubation of a 6-fold excess of $YchF_{E.coli}$ with ~0.7 μM ribosomes in the presence and absence of ATP, ADP or the non-hydrolysable ATP analog ADPNP, and subsequent centrifugation through a 10% sucrose cushion. Under these conditions only ribosomes or ribosomal subunits, free or in complex with $YchF_{E.coli}$ are able to sediment through the sucrose cushion while small molecules, like free $YchF_{E.coli}$ are retained in the supernatant. After centrifugation, the obtained ribosomal pellets were dissolved and analyzed using SDS-PAGE and silver staining (**Fig. 4A**; **Fig. S2**). Consistent with previous co-sedimentation assays using crude ribosomes,[7] $YchF_{E.coli}$ was found in the ribosome pellet under all conditions tested. However, for the first time we were able to obtain quantitative information regarding differences in binding affinities of $YchF_{E.coli}$ to the ribosome and its subunits as a function of the nucleotide-bound state. Surprisingly, in all cases the $YchF_{E.coli}$ band on the gel was significantly less intense than the ribosomal protein bands, indicative for sub-stoichiometric binding of $YchF_{E.coli}$ to 70S ribosomes or its subunits (**Fig. S2**). Furthermore, comparison of the intensity of the $YchF_{E.coli}$ band among the different nucleotide-bound states (**Fig. 4A and B**; **Fig. S2**) indicates that $YchF_{E.coli}$ binding to 70S ribosomes is modulated by the identity of the nucleotide present. Strongest binding to 70S ribosomes occurs by $YchF_{E.coli}$ in its ADPNP-bound form, followed by the ATP-bound form (comparable for both the 70S ribosome and its 50S subunit). Surprisingly, binding to the 50S subunit is very weak by $YchF_{E.coli}$ in the ADPNP-bound form and comparable to the ADP-bound form. Weak binding independent of the nucleotide is observed for all interactions with the 30S ribosomal subunit. Taken together our results indicate that $YchF_{E.coli}$ is capable to bind directly to vacant ribosomes in vitro and that this interaction is modulated by its nucleotide-bound state.

Based on the observation that strongest binding was observed only for $YchF_{E.coli}$•ADPNP and the 70S ribosome, we performed a binding titration by incubating constant concentrations of 70S ribosomes with increasing concentrations of $YchF_{E.coli}$ in the presence of ADPNP using the ribosome sedimentation assay (**Fig. 4C**). We quantified the fraction of 70S ribosomes that bound $YchF_{E.coli}$ using densitometry (Materials and Methods) and plotted the average values obtained from three independent experiments against the respective YchF concentration. Fitting with a hyperbolic function (**Fig. 4D**) allowed us to determine the maximal binding stoichiometry (B_{max}) and binding affinity (K_D) of the 70S ribosome for $YchF_{E.coli}$•ADPNP (Materials and Methods). YchF binding to 70S saturates at a binding stoichiometry of 0.30 ± 0.04 to 1, suggesting that only 30% of the ribosomes from the total 70S population are capable of forming a tight binding interaction with $YchF_{E.coli}$•ADPNP. The resulting K_D for the $YchF_{E.coli}$•ADPNP 70S ribosome interaction is 3.3 ± 1.0 μM, comparable to affinities of other ribosome binding proteins (*E. coli* trigger factor•70S, K_D = 1.1 μM;[41] *Sulfolobus solfataricus* twin-ATPase ABCE1•ADPNP•30S, K_D = 1 μM).[42]

Michalis-Menten analysis of YchF's intrinsic ATPase activity. Although previous studies have reported that YchF preferentially hydrolyzes ATP over GTP,[6,19,23,27,28,34] little is known about the catalytic properties of this intrinsic ATPase activity. To this end, we first wanted to confirm that $YchF_{E.coli}$ is indeed capable of hydrolyzing ATP more efficiently than GTP. Therefore, 5 μM YchF was incubated with an excess (75 μM) of [γ-^{32}P]-ATP or increasing concentrations (15 μM, 75 μM and 125 μM) of [γ-^{32}P]-GTP at 37°C. Multiple turnover hydrolysis activity was followed by quantifying the liberated inorganic phosphate over time using scintillation counting (**Fig. 5A**), confirming that only ATP was efficiently hydrolyzed, but not GTP (**Fig. 5A**). Based on this, we then proceeded to determine the Michaelis-Menten parameters describing $YchF_{E.coli}$'s intrinsic ATPase activity by incubating 5 μM $YchF_{E.coli}$ with varying [γ-^{32}P]-ATP concentrations (**Fig. 5B**). Plotting the initial rates of ATP hydrolysis vs. the concentration of ATP and fitting the data with a Michaelis-Menten equation (see Materials and Methods)

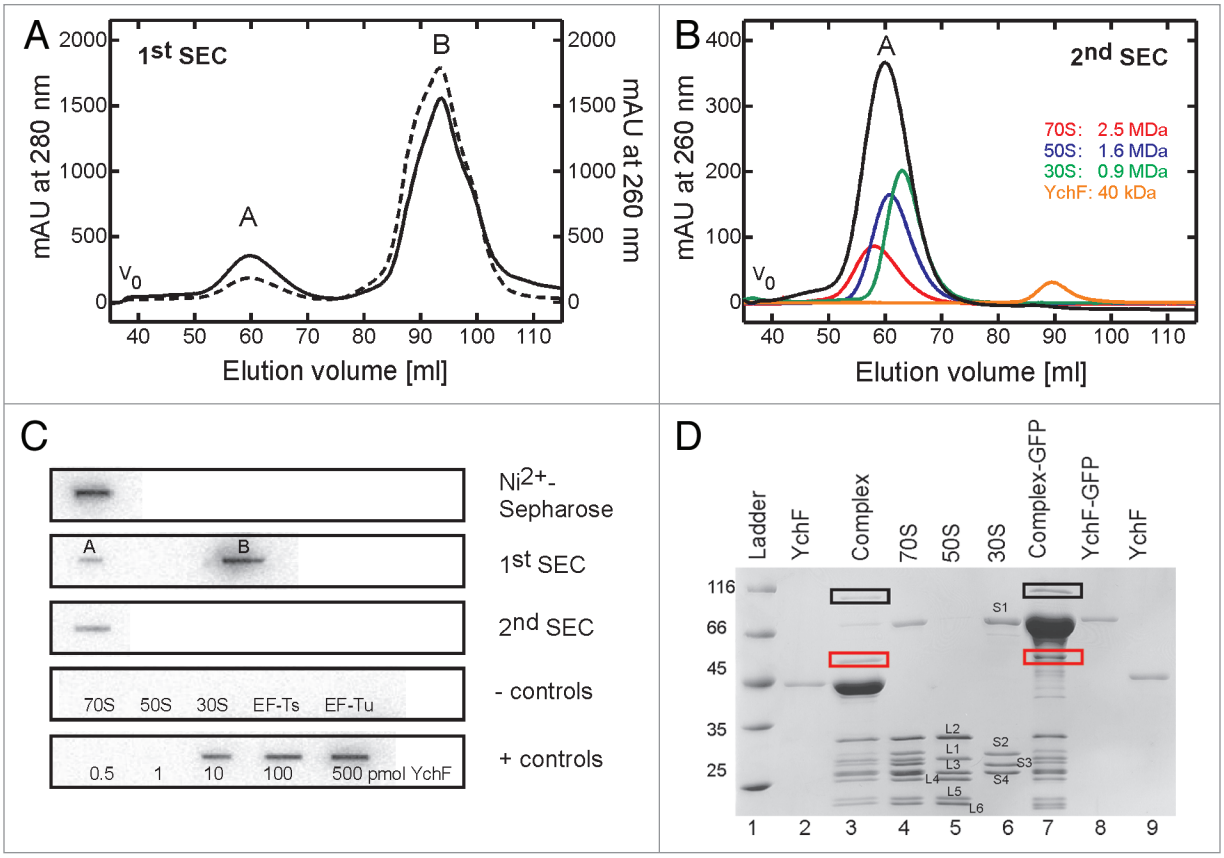

Figure 3. Co-purification of YchF and 70S ribosomes. (**A**) Protein from an initial Ni^{2+}-Sepharose pull-down of His-tagged YchF was concentrated and analyzed using a Sephacryl S400 size exclusion column equilibrated in $TAKM_7$ (pH 7.5) with 1 mM DTT as the elution buffer. The absorbance in milli Absobtion Units (mAU) at 260 nm (——) and 280 nm (– – –) was detected and two peaks (**A** and **B**) were observed in the chromatogram. The void volume V_0 of the column is approximately 35 mL. (**B**) Analysis of peak A by a second round of size exclusion chromatography using Sephacryl S400 and detection at 260 nm (black). For comparison the column was calibrated with 30 pmol of purified 70S (red), 50S (blue) and 30S (green) ribosomes and with 32,000 pmol purified YchF (orange). (**C**) Slot-blot analysis of different purification steps and immuno-detection using an anti-YchF antibody. Row 1: 10 µL of pooled eluate after a Ni^{2+}-Sepharose pull-down (~500 pmol YchF); Row 2: ~10 pmol of the high molecular weight complex (peak A) after the first SEC and ~700 pmol of SEC peak B (based based on absorbance at 260 nm/280 nm and the extinction coefficient for 70S ribosomes and YchF, respectively); Row 3: ~10 pmol of the high molecular weight complex (peak A); Row 4: negative controls, ~100 pmol of purified 70S, 50S and 30S ribosomes and ~1000 pmol of the elongation factors Ts (EF-Ts) and Tu (EF-Tu); Row 5: positive controls, increasing amounts (as indicated) of purified YchF. (**D**) Analysis of the high molecular weight complex (Peak A) by 15% SDS-PAGE and Coomassie blue staining - 7.5 pmol of Peak A from the second SEC after wild-type YchF pull-down (complex) and 7.5 pmol of Peak A from the second SEC of a YchF-GFP fusion construct (complex-GFP); 7.5 pmol purified 70S, 50S and 30S ribosomes, 10 pmol purified YchF and YchF-GFP (indicated respectively) were loaded for comparision. Bands subsequently identified as 2-oxoglutarate dehydrogenase and RhlE are indicated by black and red boxes, respectively.

revealed a maximal rate of ATP hydrolysis ($v_{max,\ ATP}$) of 1.8 ± 0.1 µM min^{-1}. Given the experimental conditions, this results in a $k_{cat,\ ATP}$ of 0.36 ± 0.02 min^{-1}. This turnover number is similar to ATP-hydrolysis rates of YchF from *H. influenza* ($k_{cat,\ ATP}$ = 0.1 min^{-1}), *S. cerevisae* (Ybr025c / Ola1p, $k_{cat,\ ATP}$ = 0.08 min^{-1}) and *H. sapiens* (hOLA1, $k_{cat,\ ATP}$ = 0.05 min^{-1}) determined previously under comparable conditions.[28]

In contrast to previous studies reporting only a specific ATPase activity for $YchF_{E.coli}$,[7] we also determined the Michaelis-Menten constant for ATP ($K_{M,\ ATP}$, **Fig. 5B**). Interestingly, we find that the $K_{M,\ ATP}$ of 41.3 ± 5.8 µM is significantly higher than the K_D of 0.9 µM for mant-ATP determined in this study. The K_M only equals the K_D (= k_{-1}/k_1) for the classical Michaelis-Menten mechanism were the catalytic rate (k_{cat}) is significantly slower than the substrate dissociation (k_{-1}).[43] For $YchF_{E.coli}$, and most other enzymes, the K_M is influenced not only by the rate constants for substrate binding (k_1, k_{-1}), but also by the rate constant of catalysis (k_{cat}) or other subsequent steps. While the exact kinetic mechanism of ATP hydrolysis by the HAS-GTPase YchF is not known, our data are consistent with a Briggs-Haldane mechanism where the rate constant of catalysis (k_2) is comparable to substrate dissociation (k_{-1}) and therefore $K_M = (k_{-1} + k_2) / k_1$.[43] As $YchF_{E.coli}$ has a high catalytic constant (k_{cat} = 0.36 ± 0.02 min^{-1}) when compared with other translational GTPases, most likely reflecting the rate constant of catalysis (k_2), it is therefore likely that this rate constant of catalysis influences the K_M and increases it relative to the K_D. The catalytic parameters of $YchF_{E.coli}$ are summarized in **Table 2**.

The 70S ribosome stimulates the ATPase activity of YchF in vitro. Based on our observation that $YchF_{E.coli}$ is capable of

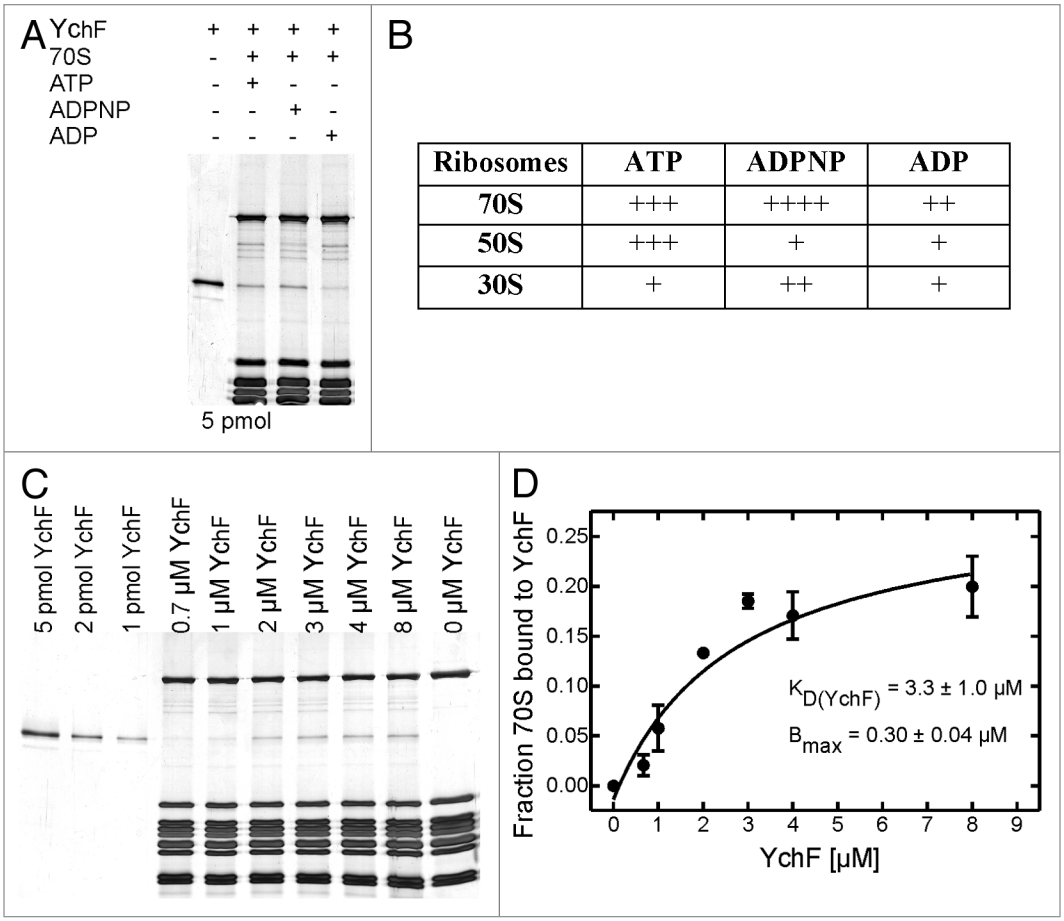

Figure 4. In vitro binding of YchF to ribosomes and ribosomal subunits. (**A**) Complexes of purified components were formed by incubating 4 µM YchF, 0.68 µM 70S, 50S or 30S ribosomes in TAKM$_7$ (pH 7.5) at cellular concentrations (2 mM) of ATP, ADP or the non-hydrolyzable ATP analog ADPNP for 15 min at 37°C. Samples were then loaded onto a 10% sucrose cushion and ribosomes were pelleted by ultracentrifugation. Five pmol ribosomes were analyzed by SDS-PAGE and silver staining. In lane one of the SDS-PAGE 5 pmol of YchF were loaded for comparison. (**B**) Qualitative summary of ribosome pelleting experiments performed under various conditions. (**C**) Determination of the equilibrium dissociation constant (K_D) of YchF and 70S ribosomes in the presence of ADPNP. Increasing concentrations of YchF were incubated with 0.68 µM 70S ribosomes and 2 mM ADPNP at 37°C for 15 min. 70S ribosomes were pelleted and analyzed as described above. In the first three lanes of the gel different amounts of purified YchF were loaded as a standard. The other lanes contain 5 pmol 70S ribosomes after pelleting. The fraction of ribosomes bound to YchF was determined by measuring the intensities of three ribosomal protein bands and the YchF band with ImageJ. (**D**) The resulting binding curve from plotting the fraction of 70S ribosomes bound to YchF vs. the YchF concentration was fit with a hyperbolic function to yield a K_D of 3.3 ± 1.0 µM and a binding stochiometry of 0.3 to 1.

forming complexes with purified 70S, 50S and 30S ribosomes in vitro, we next tested if ribosomes are able to affect the enzymatic activity of the protein and might act as an ATPase activating factor (AAF, in analogy to the GTPase activating factor GAF). To this end, ATP hydrolysis of YchF in the presence and absence of ribosomes was measured under multiple turnover conditions. One µM YchF was incubated with 125 µM [γ-^{32}P]-ATP and 5 µM 70S, 50S or 30S ribosomes at 37°C, samples were taken at different time points and the amount of liberated inorganic phosphate was determined by scintillation counting. Only in the presence of 70S ribosomes, YchF$_{E.coli}$ (**Fig. 6A**) exhibited a significant increase in the observed rate of ATP hydrolysis, whereas 30S and 50S ribosomal subunits had no effect.

To further characterize the 70S-stimulated ATPase activity of YchF$_{E.coli}$, we performed a Michaelis-Menten titration by measuring the initial velocities of ATP hydrolysis at 1 µM YchF$_{E.coli}$, 125 µM [γ-^{32}P]-ATP and varying concentrations of 70S ribosomes (**Fig. 6B**). The resulting k_{cat} for YchF$_{E.coli}$ on the ribosome is $k_{cat, ATP, 70S}$ = 3.1 ± 0.2 min^{-1} and the corresponding Michaelis-Menten constant ($K_{M, 70S}$) is 7.7 ± 1.1 µM. The latter value is in good agreement with the dissociation constant of 70S for YchF$_{E.coli}$ (3.3 ± 1.0 µM) determined in the ribosome sedimentation assay (*vide supra*), suggesting that k_{-1} is fast relative to the catalytic rate constant ($k_{cat, ATP, 70S}$). Comparing the $k_{cat, ATP}$ of YchF$_{E.coli}$ for the intrinsic hydrolysis reaction ($k_{cat, ATP}$ = 0.36 ± 0.02 min^{-1}) with the 70S ribosome stimulated reaction ($k_{cat, ATP, 70S}$ = 3.1 ± 0.2 min^{-1}) reveals that 70S ribosomes stimulate YchF$_{E.coli}$'s ATPase activity ~10-fold.

Discussion

YchF$_{E. coli}$ binds purine di- and triphosphates. To complete the available biochemical data with respect to the nucleotide affinities of a bacterial YchF and to predict the cellular state of YchF in prokaryotes (*E. coli*), ultimately instructing the identification of

functional YchF-complexes, we have determined the equilibrium-binding constants (K_D) for $YchF_{E.\ coli}$ and purine nucleotides. The obtained dissociation constants for adenine nucleotides are in the low micromolar range where as the affinities of YchF for guanine nucleotides are ~10-fold lower. Given the concentration of YchF in the *E. coli* cytosol during exponential growth of about 3.8 μM (calculated based on refs 44 and 45), the cellular concentration of purine nucleotides during mid-log growth (ATP = 3600 μM, ADP = 120 μM, GTP = 1700 μM, GDP = 200 μM),[40] and the respective K_Ds of $YchF_{E.coli}$ determined in the present study (**Table 1**), $YchF_{E.coli}$ is almost completely saturated with ATP (99%) in vivo. Only a very small fraction of the protein is bound to ADP (0.7%) and almost no nucleotide-free, GTP- or GDP-bound $YchF_{E.coli}$ is present under these conditions in the cell, underpinning YchF's function as adenine nucleotide binding protein. Interestingly, as the ratio of ATP to ADP can undergo major fluctuations in the cell (e.g., during starvation), the small difference in YchF's K_Ds for ATP and ADP could couple YchF's functional state to the cellular ATP/ADP ratio as a possible mechanism for regulating YchF's function.

Nucleotide binding induces different conformational states of $YchF_{E.coli}$. The performed equilibrium fluorescence titrations revealed that only binding of ADP but not ATP caused a decrease in YchF's intrinsic tryptophan fluorescence. However, using mant-labeled nucleotides we confirmed that $YchF_{E.coli}$ is able to bind both ADP and ATP and that the lack of a change in tryptophan fluorescence upon ATP binding likely reflects the existence of two different conformational states with characteristic fluorescence properties. This is consistent with the observation that the available X-ray structures of the *apo* form of YchF, as well as hOla bound to the non-hydrolysable ATP-analog ADPCP, reveal no conformational change. In contrast to ATP/ADPCP, binding of the non-hydrolysable ATP-analog ADPNP to $YchF_{E.coli}$ leads to a small change in the intrinsic fluorescence that might be the result of the structural differences between ADPNP and ATP/ADPCP, inducing a slightly different conformation in the protein. The existence of YchF in two structurally and functionally different conformations, ATP/*apo* vs. ADP, is supported by the different affinities of the respective complexes/conformation for the 70S ribosome, suggesting a conformational change upon nucleotide binding as part of the functional cycle of YchF.

Interestingly, we observed significantly different amplitudes for the changes in tryptophan fluorescence upon binding of guanine nucleotides when compared with the adenine nucleotide titrations. This could either be due to the existence of a different guanine nucleotide (GDP and GTP) specific conformational state or distinct binding sites with different tryptophan-fluorescence quenching properties. Alternatively, guanine nucleotides might bind to a second nucleotide/nucleic acid binding site at the inner surface of YchF's cleft (**Fig. 1**). Further experiments will be necessary to confirm this hypothesis.

Interaction of YchF and the ribosome in vivio and in vitro. In order to characterize the cellular interaction partners of $YchF_{E.coli}$, we performed a Ni^{2+}-Sepharose pull-down experiment revealing that $YchF_{E.coli}$ is part of a high molecular weight complex in vivo containing 70S ribosomes and two additional proteins,

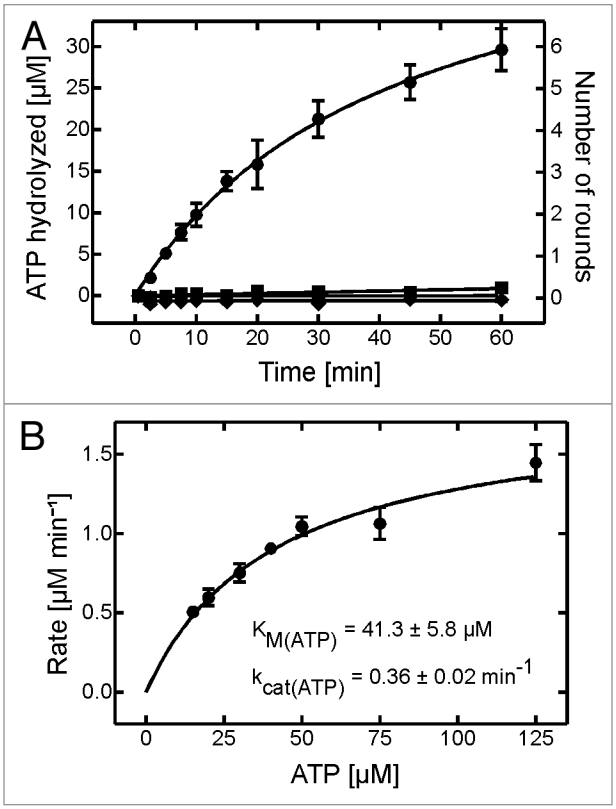

Figure 5. Intrinsic NTPase activity of YchF. (**A**) 5 μM YchF was incubated with 75 μM [γ-^{32}P]-ATP (●), 15 μM [γ-^{32}P]-GTP (▲), 75 μM [γ-^{32}P]-GTP (■), or 125 μM [γ-^{32}P]-GTP (◆) at 37°C. Samples were taken after different time points and liberated γ-^{32}Pi was extracted and subsequently quantified by scintillation counting. (**B**) Michaelis-Menten titration of 5 μM YchF and increasing concentrations of [γ-^{32}P]-ATP. Initial rates were plotted against the ATP concentration and fit with a hyperbolic function to yield the catalytic constants v_{max} of 1.8 ± 0.1 μM min^{-1} and K_M of 41.3 ± 5.8 μM.

Table 2. Michaelis-Menten kinetic parameters of *E. coli* YchF

	v_{max} [μM*min^{-1}]	K_M [μM]	k_{cat} [min^{-1}]
YchF + ATP	1.8 ± 0.1	41.3 ± 5.8	0.36 ± 0.02
YchF•ATP + 70S	3.1 ± 0.2	7.7 ± 1.1	3.1 ± 0.2

the ATP-dependent RNA helicase RhlE and 2-oxoglutarate dehydrogenase. Previous studies have already pointed at an in vivo association of YchF with ribosomes in eukaryotes. Polysome profiling experiments of cell lysates from the *Trypanosoma cruzi* and immunodetection using a YchF-specific antibody indicated that *T. cruzi* YchF ($YchF_{T.cruzi}$) co-sediments with 80S, 60S and 40S ribosomes and polysomes.[6] Consistent with this is the presence of YchF in megadalton complexes from the chloroplast stroma of the plant *Arabidopsis thaliana*,[8] where YchF was found to be associated to about 6% of 70S ribosomes and polysomes (calculated based on ref. 8). A low fraction of ribosome occupancy is supported by our observation that the final yields of YchF•70S complexes from our pull-down experiments are usually very

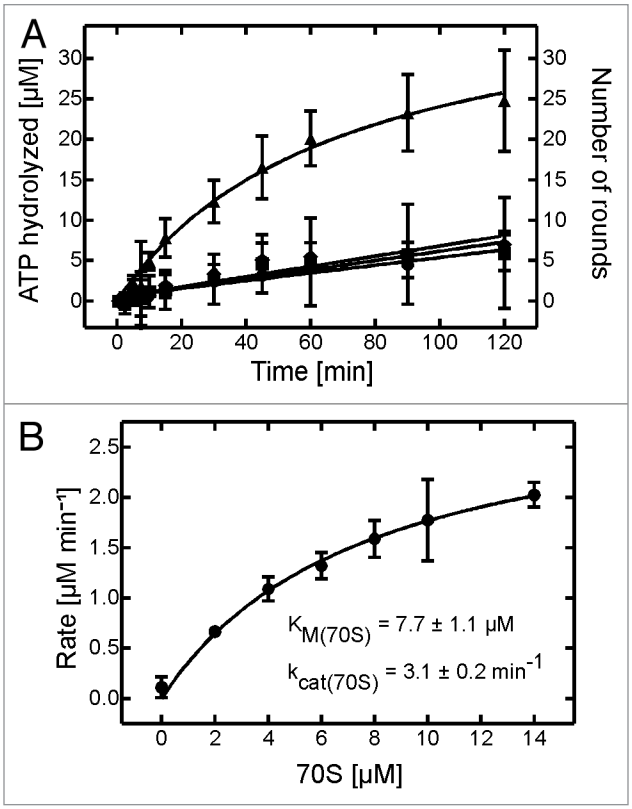

Figure 6. Ribosome-stimulated ATPase activity of YchF. (**A**) Time courses of ATP hydrolysis of 1 μM YchF and 125 μM [γ-^{32}P]-ATP in the absence (●) and presence of 5 μM 70S (▲), 5 μM 50S (■) or 5 μM 30S (◆) ribosomes. Reactions were incubated at 37°C and 5 μL aliquots were taken at different time points to follow the liberation of γ-^{32}Pi. (**B**) Michaelis-Menten titration with 70S ribosomes. One μM YchF and 125 μM [γ-^{32}P]-ATP were incubated with increasing concentrations of 70S ribosomes. 70S concentration dependence of the initial rates was fit with the Michaelis-Menten equation to obtain a v_{max} of 3.1 ± 0.2 μM min^{-1} and a K_M of 7.7 ± 1.1 μM.

low (~20 pmol/g cells). This is remarkable since the concentration of both ribosomes (~20 μM)[46] and overexpressed YchF in the cells was doubtlessly high which supports the idea that also in prokaryotes YchF only interacts with ribosomes of a specific makeup or defined functional state. The cellular occupancy of ribosomes with YchF lies in a similar range as the occupancy of ribosomes with initiation factor 3 (IF-3), trigger factor or the ribosome biogenesis factors EngA and Era. Furthermore, the cellular concentration of native YchF in *E. coli* is about 3.8 μM (vide supra) which lies in the same range as the concentration of other ribosome-interacting factors like IF-2 (8.4 μM), FtsY (1.7 μM), EF4/LepA (2.5 μM), HflX (0.6 μM) and EngA (0.9 μM) (calculated based on refs. 44 and 45). These observations support the idea that YchF's interaction with the ribosome is a common, evolutionary-conserved feature of YchF and its homologs.

YchF binds to a subset of 70S in vitro. We were able to form stable reconstituted $YchF_{E.coli}$•70S ribosome complexes in vitro using purified components, consistent with our findings from the in vivo pull-down and demonstrating that the 70S ribosome alone is an interaction partner of $YchF_{E.coli}$, as YchF binding is independent of RhlE and 2-oxoglutarate dehydrogenase. Based on our detailed understanding of the nucleotide binding properties of $YchF_{E.coli}$, we were also able to demonstrate that purified $YchF_{E.coli}$ is capable of binding to the 70S ribosome and its subunits (30S and 50S), that binding of YchF is different for the ribosome and its subunits, and that binding depends on the nucleotide-bound state of the protein. Our observation that the $YchF_{E.coli}$-30S interaction is significantly weaker than for 70S and 50S might explain why 30S-bound YchF or any subtle variations in the interaction with the ribosome and the 50S subunit might have not been reported in previous studies.[7] Furthermore, the use of purified ribosomes also enabled the observation that YchF binds to only ~30% of the 70S ribosomes in the total pool of purified ribosomes, raising the question of what makes these ribosomes different. Consistent with the idea of a role for YchF in ribosome maturation, one could speculate that a fraction of the purified 70S ribosomes may represent very late intermediates during ribosome biogenesis. Srivastava and Schleissinger reported that the final step in maturation of 23S rRNA occurs during ongoing protein synthesis, i.e., when polysomes or initiation complexes are assembled.[47] Because of their similar molecular weight and the fact that the cells from which the ribosomes were isolated were in mid-log phase, such late pre-ribosomes might have co-purified with mature 70S ribosomes during the zonal purification.

The 70S ribosome stimulates the ATPase activity of YchF in vitro. Based on our observation that $YchF_{E.coli}$ will be completely saturated with ATP under cellular conditions, we performed a Michaelis-Menten analysis of YchF with ATP to characterize the enzymatic parameters of the protein ($k_{cat,\ ATP}$ of 0.36 ± 0.02 min^{-1} and a $K_{M,\ ATP}$ of 41.3 ± 5.8 μM). Interestingly, the K_D of YchF for ATP is significantly smaller (K_D = 0.9 μM) than the $K_{M,\ ATP}$, suggesting that steps after binding of ATP to YchF, like k_{cat} or product release might influence the K_M. Compared with the other universally conserved NTPases studied so far, $YchF_{E.coli}$ has the highest turnover number (**Table S1**). However, YchF's $k_{cat,\ ATP}$ is low when compared with other ribosome associated GTPases (RA-GTPases), but similar to catalytic rates of other HAS-NTPases (**Table S2**). The successful in vitro reconstitution of $YchF_{E.coli}$•ribosome complexes using highly purified 70S ribosomes enabled us to show for the first time that 70S ribosomes (but not the 50S or the 30S ribosomal subunits) are able to stimulate $YchF_{E.coli}$'s intrinsic ATPase activity by about 10-fold ($k_{cat,\ ATP\ 70S}$ = 3.1 min^{-1}). Although a 10-fold stimulation is low when compared with other translational GTPases such as translation factors EF-Tu (5,000,000× to 50,000,000× stimulation)[48] or EF-G (17,000,000 × stimulation)[49] (**Table S1**), it is quite similar to the effect that the respective GAF's have on other HAS-GTPase like FeoB (22-fold stimulation),[50] MmnE (30-fold stimulation),[32,51,52] or ATPases like the RNA-helicase Mss116 (7-fold stimulation).[53] The 70S ribosome therefore represents the first functionaly confirmed interaction partner of $YchF_{E.coli}$ and acts as an ATPase activating factor (AAF). Based on the universality of YchF's interaction with the ribosome, this is likely also true for other prokaryotic and eukaryotic YchF homologs.

Minimal functional model. Based on our data, we suggest a minimal model for $YchF_{E.\ coli}$'s functional cycle (**Fig. 7**) to guide the unraveling of YchF's cellular role and a complete functional cycle. YchF in its ATP-bound conformation binds to a specific state of the 70S ribosome (70S*). These 70S* represent a state of the ribosome likely to exist in all organisms, as YchF proteins are highly conserved and found throughout all domains of life. Interaction with the 70S* stimulates YchF's ATPase activity and ATP is hydrolyzed to ADP. YchF undergoes a conformational change to the ADP-conformation. In its ADP-bound state, YchF has a lower affinity for the 70S* and dissociates. Finally, the ADP dissociates from YchF. Due to the high cellular concentration of ATP, YchF•ATP is regenerated and competent for another round of 70S* binding and catalysis. The proposed minimal cycle leads to a futile consumption of ATP, suggesting that states of the ribosome or additional factors such as proteins or RNAs exist that are able to modulate the ATPase activity of YchF. Furthermore, we need to answer the question with respect to the state that YchF might induce in the ribosome upon ATP hydrolysis (e.g., displacement of other ribosome biogenesis factors or protection of the ribosome during its synthesis).

In summary. Results presented here demonstrate that YchF from *E. coli* binds to 70S ribosomes in vivo and in vitro. Furthermore, we show for the first time that YchF exists in two different nucleotide-dependent conformations and that the 70S ribosome is capable of stimulating YchF's ATPase activity, acting as a ATPase activating factor (AAF). We therefore report the first detailed biochemically characterized functional interaction of YchF with a cellular component, enabling us to devise a first minimal mechanistic model for its functional cycle. Our results support a role of YchF in protein synthesis, maybe by regulating ribosome function or ribosome biogenesis.

Materials and Methods

All solvents and biochemical reagents have been purchased from Sigma-Aldrich, VWR, BioBasic Inc. and Fisher Scientific unless otherwise noted. All enzymes required for the construction of site-specific modified genes were purchased from New England Biolabs and Fermentas. Oligonucleotides used for gene cloning were purchased from Integrated DNA Technologies. Radiochemicals were purchased from MP Biomedicals and N-methylanthraniloyl (mant)-labeled nucleotides from Invitrogen or Jena Bioscience. *E. coli* MRE600 cells were purchased from the Fermentation Facility of the University of Alabama at Birmingham.

Cloning and expression. The coding region of the *ychf* gene from *E. coli* was PCR-amplified from genomic DNA using primers (5'-TTT AAA TCA TGG GAT TCA AAT GC-3' and 5'-GCA GAT TAA TTC GAA AAC AGA GTA CTC C-3') and Phusion polymerase (Thermo Fisher Scientific; Cat. No. F-530L). The PCR products were purified and ligated into SmaI digested pUC19 (Invitrogen; Cat. No. 15364–011) (T4 DNA ligase, Invitrogen; Cat. No. 15224–017). After the ligation mixture was transformed into *E. coli* DH5α cells (New England Biolabs; Cat. No. C2987I), positive clones were selected and the open reading frame was digested with BamHI and

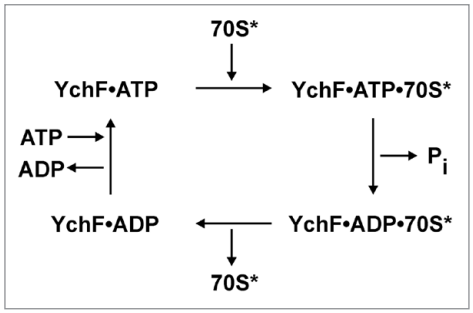

Figure 7. Minimal Model of YchF function: YchF in its compact ATP-bound state binds to certain "special" 70S ribosomes (70S*). Interaction with 70S* stimulates YchF's ATPase activity and ATP is hydrolyzed to ADP. In its open ADP-bound state YchF has a lower affinity for 70S* and dissociates. Subsequently, YchF is recharged with ATP and becomes competent for another round of 70S* binding and catalysis.

*Hind*III and ligated into similarly-digested pET28a expression vector (EMD; Cat. No. 69864–3) to generate an N-terminally His-tagged YchF protein. Positive clones were confirmed by restriction mapping and DNA sequencing (Genewiz).

The resulting recombinant plasmid was transformed into the *E. coli* B strain BL21-DE3 (Invitrogen; Cat. No. C6000-03) for YchF overexpression. Overnight cultures of transformed cells were grown in Luria Bertani medium (10 g tryptone, 5 g yeast extract, 10 g NaCl in 1 L H_2O, pH 7.5) supplemented with 50 μg/mL kanamycin at 37°C and used to inoculate expression cultures to an OD_{600} of 0.1. When the cell density reached an OD_{600} of approximately 0.6, overexpression was induced by the addition of Isopropyl β-D-1-thiogalactopyranoside (IPTG) to a final concentration of 1 mM. After induction, cells were grown for 3 h and then harvested by centrifugation at 5,000 × g for 10 min. The cell pellet was flash frozen in liquid nitrogen and stored at -80°C until needed.

We used a clone from the ASKA library, a set of clones in which every single predicted ORF of the *E. coli* K12 strain AG1 was individually transferred into an expression vector.[36] Thereby the gene product was linked to a His-tag and seven spacer amino acids at its N-terminal end and five spacer amino acids and the green fluorescence protein (GFP) at its C-terminal end. The resultant plasmid vector pCA24N carries a chloramphenicol resistance gene and the IPTG-inducible promoter $P_{T5\text{-}lac}$ which regulated expression of the YchF-GFP fusion protein.

The fusion construct was overexpressed in *E. coli* K12 AG1 cells as described above for the overexpression of wild-type YchF in *E. coli* BL21-DE3 except that the LB-medium contained 30 μg/mL chloramphenicol and no kanamycin.

Purification of His-tagged YchF and YchF-GFP. All purification steps were performed at 4°C. The harvested frozen cell pellet from the overexpression was thawed on ice and resuspended in 7 mL opening/binding buffer [50 mM Tris-Cl pH 7.5, 60 mM NH_4Cl, 7 mM $MgCl_2$, 7 mM β-mercaptoethanol, 1 mM phenylmethylsulfonyl fluoride (PMSF), 300 mM KCl, 10 mM imidazole, 15% glycerol, 150 μM ADP] per gram of cells. While stirring on ice for 1 h, lysozyme was added to a final concentration of 1 mg/mL per gram of cells. Subsequently 12.5 mg sodium

deoxycholate per gram of cells and a few crystals of DNase I were added and the mixture was stirred further for 30 min prior to centrifugation at 3,000 × g for 30 min and then 20,000 × g for 1 h in a Beckman J2–21M centrifuge using a JA-20 rotor. The resulting cleared cell lysate was applied to a 5 mL Ni^{2+}-Sepharose column (GE Healthcare; Cat. No. 17–5318–02) and His-tagged protein was allowed to bind to the resin for 1 h. Unbound protein was washed away with 18 column volumes of binding buffer and 24 column volumes of binding buffer containing 20 mM imidazole. Resin-bound protein was then eluted with 10 column volumes of binding buffer containing 250 mM imidazole. The protein was concentrated and the buffer exchanged with Q-Sepharose buffer A [50 mM Tris-Cl pH 7.5, 10 mM $MgCl_2$, 5 mM EDTA, 1 mM dithiothreitol (DTT)] using a Vivaspin 20 (30,000 MWCO) (GE Healthcare; Cat. No. 28–9323–61). Further purification was done using a Q-Sepharose XK26/10 Fast Flow (GE Healthcare; Cat. No. 17–0510–10) anion-exchange column on an Äkta FPLC purification system (GE Healthcare) employing a salt gradient form 0% buffer A (50 mM Tris-Cl pH 7.5, 10 mM $MgCl_2$, 5 mM EDTA, 1 mM DTT) to 100% buffer B (50 mM Tris-Cl pH 7.6, 10 mM $MgCl_2$, 5 mM EDTA, 1M KCl, 1 mM DTT). Fractions containing YchF were pooled, concentrated and loaded onto a Superdex 75 XK26/100 column (GE Healthcare; Cat. No. 17–1044–02) equilibrated in final storage buffer $TAKM_7$ (50 mM Tris-Cl 7.5, 70 mM NH_4Cl, 30 mM KCl, 7 mM $MgCl_2$) with 1 mM DTT. The elution fractions were analyzed by SDS-PAGE and stained with Coomassie blue or electroblotting onto BioTrace nitrocellulose transfer membrane (Pall Corporation; Cat. No 66485) for Western-blot analysis.

Fractions containing pure YchF or YchF-GFP were pooled, concentrated, flash-frozen in liquid nitrogen and stored at -80°C. Protein concentrations were determined photometrically using Beers-law by measuring the absorbance at 280 nm and the theoretical molar extinction coefficients of 16,305 M^{-1} cm^{-1} for wild-type YchF and 37,820 M^{-1} cm^{-1} for the YchF-GFP fusion protein. Extinction coefficients were calculated based on the amino acid composition with ProtPram.[54]

Western-blotting, Slot-blotting and Immuno-detection. Electroblotting was performed in transfer buffer (48 mM Tris-Cl pH 9.2, 39 mM glycine, 0.037% SDS) at 100 V over night at 4°C. Slot-blotting samples were directly spotted onto a nitrocellulose membrane washed with TBS (10 mM Tris-Cl pH 7.5, 150 mM NaCl). Membranes were stained with 2% Ponceau S (Bio-Rad Protein assay dye reagent concentrate, Bio-Rad; Cat. No. 500–0006) to confirm blotting. After destaining, the membrane was blocked with 3% (w/v) skimmed milk in TBS for 1 h. Subsequently, the membrane was incubated with a 1:6,000 dilution of either monoclonal mouse His-Tag antibody or polyclonal rabbit YchF antibody (Pacific Immunology) for at least 1 h at room temperature and then washed three times with TTBS (10 mM Tris-Cl pH 7.5, 150 mM NaCl, 0.05% Tween-20). Incubation with 1:6,000 dilution of either goat anti-mouse or goat anti-rabbit horseradish peroxidase conjugated antibody was done for 1 h followed by stringent washing with TTBS. Detection was performed using 0.01% p-coumaric acid, 0.01% luminol and 0.03% H_2O_2 in 1 M Tris-Cl pH 8.0 in a Typhoon Trio scanner (GE Healthcare).

Identification of YchF's cellular interaction partners. To identify potential interaction partners of YchF and YchF-GFP, pull-down experiments were performed by overexpressing recombinant N-terminally His-tagged YchF or YchF-GFP in *E. coli* and subsequently capturing the in vivo formed complexes by binding to a Ni^{2+}-Sepharose resin. Overexpression of the protein, cell-opening and binding to and elution from the Ni^{2+}-Sepharose column was done as described above. Eluates from the Ni^{2+}-Sepharose resin were pooled and protein was concentrated and loaded onto a 16/60 (120 mL) HiPrep Sephacryl S400 HR size exclusion column (GE Healthcare, Cat. No. 28–9356–04) pre-equilibrated with $TAKM_7$ with 1 mM DTT using an Äkta FPLC system (GE Healthcare). According to the manufactures specifications the separation range of the Sephacryl S400 is 20 kDa to 8 MDa. Absorbance at 260 nm and 280 nm was monitored and peak fractions were pooled, concentrated and frozen in liquid nitrogen for further analysis.

The HiPrep Sephacryl S400 column was calibrated with 32,000 pmol purified YchF and 30 pmol of purified 70S, 50S and 30S ribosomes in $TAKM_7$ with 1 mM DTT. In addition, 0.5 μm polystyrene microspheres (Polysciences, Inc., Cat. No. 07307–15) were utilized to determine the void volume of the column. Therefore, it was equilibrated with Polybead buffer (10 mM Tris-Cl pH 8.0 at room temperature (RT), 50 mM NaCl, 0.01% Tween 80 (Polysorbate 80) at RT and 40 μL of the original Polybead stock diluted in 60 μL Polybead buffer was loaded and run at 0.5 mL/min while detecting the absorbance at 254 nm.

Preparation of ribosomes and rRNAs. Bacterial ribosomes were prepared as described.[55] Briefly, frozen *E. coli* MR600 cells were opened by alumina grinding in cell opening buffer (20 mM Tris-Cl pH 7.6, 100 mM NH_4Cl, 10.5 mM $MgCl_2$, 0.5 mM EDTA, 3 mM β-mercaptoethanol). A few crystals of DNase I were added prior to centrifugation for 30 min at 30,000 × g using a Beckman JA-14 rotor (Beckman Coulter Canada, Inc.) in a Beckman J2–21M centrifuge (S-30 fraction). The S-30 fraction was layered onto a sucrose cushion (20 mM Tris-Cl pH 7.6, 500 mM NH_4Cl, 10.5 mM $MgCl_2$, 0.5 mM EDTA, 1.1 M sucrose, 3 mM β-mercaptoethanol) and centrifuged at 186,000 × g for approximately 17 h using a Ti45 rotor in a Beckman Optima XL-100K ultracentrifuge. The resulting ribosome pellets were rinsed and dissolved in washing buffer (20 mM Tris-Cl pH 7.6, 500 mM NH_4Cl, 10.5 mM $MgCl_2$, 0.5 mM EDTA, 7 mM β-mercaptoethanol), loaded onto a sucrose cushion and again spun for approximately 17 h at 186,000 × g. Pellets were rinsed and resuspended in washing buffer for final ultracentrifugation through a sucrose cushion at 141,000 × g for approximately 16 h using a SW28 rotor.

Afterwards the pellets were dissolved in overlay buffer (20 mM Tris-Cl pH 7.6, 60 mM NH_4Cl, 5.25 mM $Mg(CH_3COO)_2$, 0.25 mM EDTA, 3 mM β-mercaptoethanol) containing 5% sucrose. The ribosomal subunits were separated on a 10–40% sucrose gradient by zonal centrifugation at 74,000 × g for 19 h in a Ti-15 zonal rotor. Fractions containing 70S, 50S and 30S ribosomal subunits were individually pooled, pelleted, resuspended

in storage buffer (20 mM Tris-Cl pH 7.6, 50 mM NH_4Cl, 5 mM $MgCl_2$), flash frozen and stored at -80°C.

Ribosome concentrations were determined by measuring the absorbance at 260 nm and extinction coefficients of 3.91×10^7 M^{-1} cm^{-1} for 70S, 2.55×10^7 M^{-1} cm^{-1} for 50S and 1.37×10^7 M^{-1} cm^{-1} for 30S ribosomes.[56]

For rRNA purification, phenol:chloroform extraction and ethanol precipitation was utilized. RNA was then loaded on a 15% Urea-PAGE and electropheresis was performed at 300 V for 20 min. The samples were visualized by ethidium bromide staining.

Fluorescence measurements. All fluorescence measurements were performed using a QuantaMaster Fluorescence Spectrophotometer (Photon Technology International). Binding of nucleotides to 1 μM YchF was investigated at room temperature in $TAKM_7$ buffer utilizing regular nucleotides and fluorescent nucleotide analogs (mant-nucleotides). Nucleotides were prepared in $TAKM_7$ buffer and the pH was adjusted to 7.5 using 5 M NaOH.

YchF from *E. coli* contains one tryptophan and seven tyrosine residues. The change in YchF's intrinsic fluorescence upon nucleotide binding was monitored in a stirrable 2 mm × 10 mm quartz cuvette (18F-Q-1-MS; Starna Cells, Inc.). Therefore, YchF in $TAKM_7$ buffer was excited at a wavelength of 280 nm using a slit width of 2 nm. Emission spectra from 295 to 400 nm were monitored at a 1 nm step size through 5 nm slits. When mant-labeled nucleotides were used, YchF was excited at 274 nm (absorbance maximum of tyrosine) and emission spectra from 290 to 500 nm were recorded through 1.5 nm excitation and 5 nm emission slits and with a step size of 2 nm.

After addition of ADP, ADPNP or GDP to the YchF solution the sample was equilibrated for 1 min before the fluorescence scan was started. When nucleotide triphosphates were used the emission scan was started immediately without equilibration of the sample.

As a negative control, fluorescence was monitored for the titration of $TAKM_7$ buffer with nucleotides and all protein fluorescence spectra were corrected with this control. To determine the equilibrium dissociation constant (K_D) the fluorescence at 337 nm in case of unlabeled nucleotides or at 440 nm in case of mant-labeled nucleotides was plotted against the nucleotide concentration. Fluorescence intensities were then corrected for the dilution of the protein due to addition of nucleotide solution. Additionally, titrations with unlabeled nucleotides were also corrected for the effect of photobleaching over the time of the experiment.

K_Ds were determined by plotting the change in fluorescence at 337 nm or 440 nm (F) vs. the nucleotide concentration ([nt]) with respect to the initial fluorescence (F_0) and the amplitude of the signal change (ΔF_{max}). Data were fit with a hyperbolic binding equation [$F = F_0 + (\Delta F_{max} \times [nt]) / (K_D + [nt])$] using the TableCurve (Jandel Scientific) software. Final K_Ds and their standard deviations were calculated from at least three independent experiments.

Nucleotide hydrolysis assays. The multiple turnover nucleotide triphosphate hydrolysis (NTPase) activity of YchF was measured at 37°C in $TAKM_7$ buffer by following the formation of γ-$^{32}P_i$ from [γ-^{32}P]-ATP or [γ-^{32}P]-GTP over time. Prior to the experiment, [γ-^{32}P]-ATP and [γ-^{32}P]-GTP (200 dpm/pmol) were charged by incubation with 0.25 μg/μL pyruvate kinase (Roche Applied Science; Cat. No. 10109045001) and 3 mM phosphoenolpyruvate for 15 min at RT and then 15 min at 37°C. All other components were charged by incubation for 30 min at RT.

To determine YchF's intrinsic NTPase activity, the reactions contained 5 μM YchF and varying concentrations of [γ-^{32}P]-ATP or [γ-^{32}P]-GTP. For Michaelis-Menten titrations the ATP concentration was varied between 15 μM and 125 μM. The influence of 70S, 50S or 30S ribosomes on YchF's ATPase activity was measured using 1 μM YchF, 125 μM ATP and 5 μM ribosomes. Michaelis-Menten titrations were performed under the same conditions, however, the concentration of 70S ribosomes varied from 0 to 14 μM.

Hydrolysis reactions were started by the addition of radiolabelled-nucleotides, then 5 μL aliquots were taken at different time points and the reaction was quenched in 50 μL 1M $HClO_4$ with 3 mM K_2HPO_4. Inorganic phosphate was extracted using 300 μL 20 mM Na_2MoO_4 and 400 μL isopropyl acetate. Hydrolysis of ATP/GTP by YchF was quantified by monitoring the release of inorganic phosphate, [γ-$^{32}P_i$] from [γ-^{32}P]-ATP/[γ-^{32}P]-GTP using a Tri-Carb 2,800TR liquid scintillation analyzer.

All hydrolysis experiments were corrected for the background hydrolysis of ATP or GTP at 37°C. Furthermore, ribosomes show a low intrinsic ATPase activity, which was subtracted from experiments containing YchF and ribosomes. ATPase experiments were performed at least in triplicate to determine standard deviations.

For Michaelis-Menten titrations the initial velocity at different ATP or 70S concentrations was determined within the first 10 min of the reaction to ensure that consumption of the substrate was negligible. The nucleotide or 70S concentration dependence of YchF's ATPase rate was fit with the Michaelis-Menten equation $v = [v_{max} * (S)]/[K_M + (S)]$ to determine the parameters v_{max} and K_M.

In vitro reconstitution of YchF:ribosome complexes. YchF:ribosome complexes were formed by incubating 4 μM YchF, 0.68 μM 70S, 50S or 30S ribosomes in $TAKM_7$ with 1 mM DTT and magnesium-adjusted 2 mM ATP, ADP or ADPNP for 15 min at 37°C. Afterwards the mixtures were cooled on ice, quickly pulsed in a microcentrifuge and then layered onto a 10% sucrose cushion containing the respective nucleotide (10% sucrose, 2 mM $MgCl_2$, 2 mM ATP, ADP or ADPNP in $TAKM_7$ with 1 mM DTT). Ribosomes and associated factors were sedimented through the cushion by ultracentrifugation at 82,000 × g for 19 h in a in a Beckman Optima ultracentrifuge using a TLA-100.3 rotor.

After ultracentrifugation the supernatant was discarded and ribosomal pellets were dissolved in 50 μL $TAKM_7$. Ribosome concentrations were determined by absorbance measurements at 260 nm and same amounts of ribosomes were run on a 12% SDS-PAGE and visualized by silver staining.

To determine the equilibrium dissociation constant (K_D) of 70S ribosomes for YchF, ultracentrifugation experiments with 0.68 μM 70S, 2 mM $MgCl_2$, 2 mM ADPNP and increasing

YchF concentrations (0 to 8 μM) were performed. To quantify the fraction of ribosomes bound to YchF, band intensities of YchF and ribosomal proteins on the silver stained SDS-PAGE were evaluated using ImageJ.[57] The K_D was determined by plotting the fraction of ribosomes bound to YchF (Y) vs. the YchF concentration and fitting the data with a hyperbolic function $Y = B_{max}*(YchF)/[K_D + (YchF)]$, where B_{max} reflects the fraction of ribosomes in the total ribosome pool capable in binding to YchF.

Disclosure of Potential Conflicts of Interest

No potential conflicts of interest were disclosed.

Acknowledgments

This work was supported by the Canada Foundation for Innovation and the Canadian Institutes of Health Research. We thank Dr Richard Fahlman for mass spectrometry analysis, Dr Ute Kothe for critical reading of the manuscript and the members of H.J.W. laboratory for helpful comments and advice.

Supplemental Materials

Supplemental materials may be found here:
www.landesbioscience.com/journals/rna/article/22131

References

1. Koonin EV. Comparative genomics, minimal gene-sets and the last universal common ancestor. Nat Rev Microbiol 2003; 1:127-36; PMID:15035042; http://dx.doi.org/10.1038/nrmicro751.
2. Wittinghofer A, Vetter IR. Structure-function relationships of the G domain, a canonical switch motif. Annu Rev Biochem 2011; 80:943-71; PMID:21675921; http://dx.doi.org/10.1146/annurev-biochem-062708-134043.
3. Caldon CE, March PE. Function of the universally conserved bacterial GTPases. Curr Opin Microbiol 2003; 6:135-9; PMID:12732302; http://dx.doi.org/10.1016/S1369-5274(03)00037-7.
4. Mittenhuber G. Comparative genomics of prokaryotic GTP-binding proteins (the Era, Obg, EngA, ThdF (TrmE), YchF and YihA families) and their relationship to eukaryotic GTP-binding proteins (the DRG, ARF, RAB, RAN, RAS and RHO families). J Mol Microbiol Biotechnol 2001; 3:21-35; PMID:11200227.
5. Galperin MY, Koonin EV. 'Conserved hypothetical' proteins: prioritization of targets for experimental study. Nucleic Acids Res 2004; 32:5452-63; PMID:15479782; http://dx.doi.org/10.1093/nar/gkh885.
6. Gradia DF, Rau K, Umaki ACS, de Souza FSP, Probst CM, Correa A, et al. Characterization of a novel Obg-like ATPase in the protozoan *Trypanosoma cruzi*. Int J Parasitol 2009; 39:49-58; PMID:18713637; http://dx.doi.org/10.1016/j.ijpara.2008.05.019.
7. Tomar SK, Kumar P, Prakash B. Deciphering the catalytic machinery in a universally conserved ribosome binding ATPase YchF. Biochem Biophys Res Commun 2011; 408:459-64; PMID:21527254; http://dx.doi.org/10.1016/j.bbrc.2011.04.052.
8. Olinares PDB, Ponnala L, van Wijk KJ. Megadalton complexes in the chloroplast stroma of *Arabidopsis thaliana* characterized by size exclusion chromatography, mass spectrometry, and hierarchical clustering. Mol Cell Proteomics 2010; 9:1594-615; PMID:20423899; http://dx.doi.org/10.1074/mcp.M000038-MCP201.
9. Caldon CE, Yoong P, March PE. Evolution of a molecular switch: universal bacterial GTPases regulate ribosome function. Mol Microbiol 2001; 41:289-97; PMID:11489118; http://dx.doi.org/10.1046/j.1365-2958.2001.02536.x.
10. Leipe DD, Wolf YI, Koonin EV, Aravind L. Classification and evolution of P-loop GTPases and related ATPases. J Mol Biol 2002; 317:41-72; PMID:11916378; http://dx.doi.org/10.1006/jmbi.2001.5378.
11. Cruz-Vera LR, Galindo JM, Guarneros G. Transcriptional analysis of the gene encoding peptidyl-tRNA hydrolase in *Escherichia coli*. Microbiology 2002; 148:3457-66; PMID:12427937.
12. Rodnina MV, Stark H, Savelsbergh A, Wieden HJ, Mohr D, Matassova NB, et al. GTPases mechanisms and functions of translation factors on the ribosome. Biol Chem 2000; 381:377-87; PMID:10937868; http://dx.doi.org/10.1515/BC.2000.050.
13. Dassain M, Leroy A, Colosetti L, Carolé S, Bouché JP. A new essential gene of the 'minimal genome' affecting cell division. Biochimie 1999; 81:889-95; PMID:10572302; http://dx.doi.org/10.1016/S0300-9084(99)00207-2.
14. Prágai Z, Harwood CR. YsxC, a putative GTP-binding protein essential for growth of Bacillus subtilis 168. J Bacteriol 2000; 182:6819-23; PMID:11073929; http://dx.doi.org/10.1128/JB.182.23.6819-6823.2000.
15. Lehoux IE, Mazzulla MJ, Baker A, Petit CM. Purification and characterization of YihA, an essential GTP-binding protein from *Escherichia coli*. Protein Expr Purif 2003; 30:203-9; PMID:12880769; http://dx.doi.org/10.1016/S1046-5928(03)00107-4.
16. Polkinghorne A, Ziegler U, González-Hernández Y, Pospischil A, Timms P, Vaughan L. Chlamydophila pneumoniae HflX belongs to an uncharacterized family of conserved GTPases and associates with the Escherichia coli 50S large ribosomal subunit. Microbiology 2008; 154:3537-46; PMID:18957606; http://dx.doi.org/10.1099/mic.0.2008/022137-0.
17. Fischer JJ, Coatham ML, Bear SE, Brandon HE, De Laurentiis EI, Shields MJ, et al. The ribosome modulates the structural dynamics of the conserved GTPase HflX and triggers tight nucleotide binding. Biochimie 2012; 94:1647-59; PMID:22554723; http://dx.doi.org/10.1016/j.biochi.2012.04.016.
18. Adékambi T, Butler RW, Hanrahan F, Delcher AL, Drancourt M, Shinnick TM. Core gene set as the basis of multilocus sequence analysis of the subclass Actinobacteridae. PLoS One 2011; 6:e14792; PMID:21483493; http://dx.doi.org/10.1371/journal.pone.0014792.
19. Teplyakov A, Obmolova G, Chu SY, Toedt J, Eisenstein E, Howard AJ, et al. Crystal structure of the YchF protein reveals binding sites for GTP and nucleic acid. J Bacteriol 2003; 185:4031-7; PMID:12837776; http://dx.doi.org/10.1128/JB.185.14.4031-4037.2003.
20. Danese I, Haine V, Delrue RM, Tibor A, Lestrate P, Stevaux O, et al. The Ton system, an ABC transporter, and a universally conserved GTPase are involved in iron utilization by *Brucella melitensis* 16M. Infect Immun 2004; 72:5783-90; PMID:15385478; http://dx.doi.org/10.1128/IAI.72.10.5783-5790.2004.
21. Chen YC, Chung YT. A conserved GTPase YchF of *Vibrio vulnificus* is involved in macrophage cytotoxicity, iron acquisition, and mouse virulence. Int J Med Microbiol 2011; 301:469-74; PMID:21570909; http://dx.doi.org/10.1016/j.ijmm.2011.02.002.
22. Guerrero C, Tagwerker C, Kaiser P, Huang L. An integrated mass spectrometry-based proteomic approach: quantitative analysis of tandem affinity-purified in vivo cross-linked protein complexes (QTAX) to decipher the 26 S proteasome-interacting network. Mol Cell Proteomics 2006; 5:366-78; PMID:16284124; http://dx.doi.org/10.1074/mcp.M500303-MCP200.
23. Cheung MY, Xue Y, Zhou LA, Li MW, Sun SSM, Lam HM. An ancient P-loop GTPase in rice is regulated by a higher plant-specific regulatory protein. J Biol Chem 2010; 285:37359-69; PMID:20876569; http://dx.doi.org/10.1074/jbc.M110.172080.
24. Godon C, Lagniel G, Lee J, Buhler JM, Kieffer S, Perrot M, et al. The H_2O_2 stimulon in *Saccharomyces cerevisiae*. J Biol Chem 1998; 273:22480-9; PMID:9712873; http://dx.doi.org/10.1074/jbc.273.35.22480.
25. Zhang J, Rubio V, Lieberman MW, Shi ZZ. OLA1, an Obg-like ATPase, suppresses antioxidant response via nontranscriptional mechanisms. Proc Natl Acad Sci U S A 2009; 106:15356-61; PMID:19706404; http://dx.doi.org/10.1073/pnas.0907213106.
26. Zhang JW, Rubio V, Zheng S, Shi ZZ. Knockdown of OLA1, a regulator of oxidative stress response, inhibits motility and invasion of breast cancer cells. J Zhejiang Univ Sci B 2009; 10:796-804; PMID:19882753; http://dx.doi.org/10.1631/jzus.B0910009.
27. Sun H, Luo XQ, Montalbano J, Jin WX, Shi JX, Sheikh MS, et al. DOC45, a novel DNA damage-regulated nucleocytoplasmic ATPase that is overexpressed in multiple human malignancies. Mol Cancer Res 2010; 8:57-66; PMID:20053727; http://dx.doi.org/10.1158/1541-7786.MCR-09-0278.
28. Koller-Eichhorn R, Marquardt T, Gail R, Wittinghofer A, Kostrewa D, Kutay U, et al. Human OLA1 defines an ATPase subfamily in the Obg family of GTP-binding proteins. J Biol Chem 2007; 282:19928-37; PMID:17430889; http://dx.doi.org/10.1074/jbc.M700541200.
29. Kukimoto-Niino M, Murayama K, Shirouzu M, Kuramitsu S, Yokoyama S. Thermus thermophilus YchF GTP-binding protein. 2006; DOI:10.2210/pdb2dwq/pdb
30. Kniewel RK, Buglino JA, Lima CD. Structure of the Schizosaccharomyces pombe YchF GTPase. 2002; DOI:10.2210/pdb1ni3/pdb
31. Mishra R, Gara SK, Mishra S, Prakash B. Analysis of GTPases carrying hydrophobic amino acid substitutions in lieu of the catalytic glutamine: implications for GTP hydrolysis. Proteins 2005; 59:332-8; PMID:15726588; http://dx.doi.org/10.1002/prot.20413.
32. Scrima A, Wittinghofer A. Dimerisation-dependent GTPase reaction of MnmE: how potassium acts as GTPase-activating element. EMBO J 2006; 25:2940-51; PMID:16763562; http://dx.doi.org/10.1038/sj.emboj.7601171.
33. Ash MR, Guilfoyle A, Clarke RJ, Guss JM, Maher MJ, Jormakka M. Potassium-activated GTPase reaction in the G Protein-coupled ferrous iron transporter B. J Biol Chem 2010; 285:14594-602; PMID:20220129; http://dx.doi.org/10.1074/jbc.M110.111914.
34. Cheung MY, Zeng NY, Tong SW, Li WYF, Xue Y, Zhao KJ, et al. Constitutive expression of a rice GTPase-activating protein induces defense responses. New Phytol 2008; 179:530-45; PMID:19086295; http://dx.doi.org/10.1111/j.1469-8137.2008.02473.x.
35. Lakowicz JR. Principles of Fluorescence Spectroscopy. New York: Springer Science + Business Media, Inc., 2004.

36. Kitagawa M, Ara T, Arifuzzaman M, Ioka-Nakamichi T, Inamoto E, Toyonaga H, et al. Complete set of ORF clones of *Escherichia coli* ASKA library (a complete set of *E. coli* K-12 ORF archive): unique resources for biological research. DNA Res 2005; 12:291-9; PMID:16769691; http://dx.doi.org/10.1093/dnares/dsi012.
37. Steginsky CA, Frey PA. Escherichia coli alpha-ketoglutarate dehydrogenase complex. J Biol Chem 1984; 259:4023-6; PMID:6368556.
38. Jain C. The E. coli RhlE RNA helicase regulates the function of related RNA helicases during ribosome assembly. RNA 2008; 14:381-9; PMID:18083833; http://dx.doi.org/10.1261/rna.800308.
39. Shajani Z, Sykes MT, Williamson JR. Assembly of bacterial ribosomes. Annu Rev Biochem 2011; 80:501-26; PMID:21529161; http://dx.doi.org/10.1146/annurev-biochem-062608-160432.
40. Buckstein MH, He J, Rubin H. Characterization of nucleotide pools as a function of physiological state in *Escherichia coli.* J Bacteriol 2008; 190:718-26; PMID:17965154; http://dx.doi.org/10.1128/JB.01020-07.
41. Maier R, Eckert B, Scholz C, Lilie H, Schmid FX. Interaction of trigger factor with the ribosome. J Mol Biol 2003; 326:585-92; PMID:12559924; http://dx.doi.org/10.1016/S0022-2836(02)01427-4.
42. Barthelme D, Dinkelaker S, Albers SV, Londei P, Ermler U, Tampé R. Ribosome recycling depends on a mechanistic link between the FeS cluster domain and a conformational switch of the twin-ATPase ABCE1. Proc Natl Acad Sci U S A 2011; 108:3228-33; PMID:21292982; http://dx.doi.org/10.1073/pnas.1015953108.
43. Fersht A. Structure and mechanism in protein science: a guide to enzyme catalysis and protein folding. New York: W.H. Freeman & Company, 1998.
44. Ishihama Y, Schmidt T, Rappsilber J, Mann M, Hartl FU, Kerner MJ, et al. Protein abundance profiling of the *Escherichia coli* cytosol. BMC Genomics 2008; 9:102; PMID:18304323; http://dx.doi.org/10.1186/1471-2164-9-102.
45. Ishii N, Nakahigashi K, Baba T, Robert M, Soga T, Kanai A, et al. Multiple high-throughput analyses monitor the response of *E. coli* to perturbations. Science 2007; 316:593-7; PMID:17379776; http://dx.doi.org/10.1126/science.1132067.
46. Lill R, Crooke E, Guthrie B, Wickner W. The "trigger factor cycle" includes ribosomes, presecretory proteins and the plasma membrane. Cell 1988; 54:1013-8; PMID:3046750; http://dx.doi.org/10.1016/0092-8674(88)90116-X.
47. Srivastava AK, Schlessinger D. Coregulation of processing and translation: mature 5' termini of *Escherichia coli* 23S ribosomal RNA form in polysomes. Proc Natl Acad Sci U S A 1988; 85:7144-8; PMID:3050989; http://dx.doi.org/10.1073/pnas.85.19.7144.
48. Pape T, Wintermeyer W, Rodnina MV. Complete kinetic mechanism of elongation factor Tu-dependent binding of aminoacyl-tRNA to the A site of the *E. coli* ribosome. EMBO J 1998; 17:7490-7; PMID:9857203; http://dx.doi.org/10.1093/emboj/17.24.7490.
49. Rodnina MV, Savelsbergh A, Katunin VI, Wintermeyer W. Hydrolysis of GTP by elongation factor G drives tRNA movement on the ribosome. Nature 1997; 385:37-41; PMID:8985244; http://dx.doi.org/10.1038/385037a0.
50. Ash MR, Maher MJ, Guss JM, Jormakka M. A suite of Switch I and Switch II mutant structures from the G-protein domain of FeoB. Acta Crystallogr D Biol Crystallogr 2011; 67:973-80; PMID:22101824; http://dx.doi.org/10.1107/S0907444911039461.
51. Yim L, Martínez-Vicente M, Villarroya M, Aguado C, Knecht E, Armengod ME. The GTPase activity and C-terminal cysteine of the *Escherichia coli* MnmE protein are essential for its tRNA modifying function. J Biol Chem 2003; 278:28378-87; PMID:12730230; http://dx.doi.org/10.1074/jbc.M301381200.
52. Meyer S, Wittinghofer A, Versées W. G-domain dimerization orchestrates the tRNA wobble modification reaction in the MnmE/GidA complex. J Mol Biol 2009; 392:910-22; PMID:19591841; http://dx.doi.org/10.1016/j.jmb.2009.07.004.
53. Cao WX, Coman MM, Ding S, Henn A, Middleton ER, Bradley MJ, et al. Mechanism of Mss116 ATPase reveals functional diversity of DEAD-Box proteins. J Mol Biol 2011; 409:399-414; PMID:21501623; http://dx.doi.org/10.1016/j.jmb.2011.04.004.
54. Gasteiger E, Gattiker A, Hoogland C, Ivanyi I, Appel RD, Bairoch A. ExPASy: The proteomics server for in-depth protein knowledge and analysis. Nucleic Acids Res 2003; 31:3784-8; PMID:12824418; http://dx.doi.org/10.1093/nar/gkg563.
55. Milon P, Konevega AL, Peske F, Fabbretti A, Gualerzi CO, Rodnina MV. Transient kinetics, fluorescence, and FRET in studies of initiation of translation in bacteria. Methods Enzymol 2007; 430:1-30; PMID:17913632; http://dx.doi.org/10.1016/S0076-6879(07)30001-3.
56. Moore SD, Baker TA, Sauer RT. Forced extraction of targeted components from complex macromolecular assemblies. Proc Natl Acad Sci U S A 2008; 105:11685-90; PMID:18695246; http://dx.doi.org/10.1073/pnas.0805633105.
57. Abramoff MDM, Sunanda PJR. Image processing with ImageJ. Biophotonics international 2004; 11:36-42.
58. Arnold K, Bordoli L, Kopp J, Schwede T. The SWISS-MODEL workspace: a web-based environment for protein structure homology modelling. Bioinformatics 2006; 22:195-201; PMID:16301204; http://dx.doi.org/10.1093/bioinformatics/bti770.
59. Kiefer F, Arnold K, Künzli M, Bordoli L, Schwede T. The SWISS-MODEL Repository and associated resources. Nucleic Acids Res 2009; 37(Database issue):D387-92; PMID:18931379; http://dx.doi.org/10.1093/nar/gkn750.